

Clustering Based Adaptive Power Control for Interference Mitigation in Two-Tier Femtocell Networks

Hong Wang¹ and Rongfang Song^{1,2}

¹College of Telecommunication and Information Engineering, Nanjing University of
Posts and Telecommunications, Nanjing 210003, China
[e-mail: wanghong_1989@yahoo.com]

²National Mobile Communications Research Laboratory, Southeast University,
Nanjing 210096, China
[e-mail: songrf@njupt.edu.cn]

*Corresponding author: Rongfang Song

*Received October 8, 2013; revised December 17, 2013; revised March 6, 2014; accepted April 7, 2014;
published April 29, 2014*

Abstract

Two-tier femtocell networks, consisting of a conventional cellular network underlaid with femtocell hotspots, play an important role in the indoor coverage and capacity of cellular networks. However, the cross- and co-tier interference will cause an unacceptable quality of service (QoS) for users with universal frequency reuse. In this paper, we propose a novel downlink interference mitigation strategy for spectrum-shared two-tier femtocell networks. The proposed solution is composed of three parts. The first is femtocells clustering, which maximizes the distance between femtocells using the same slot resource to mitigate co-tier interference. The second is to assign macrocell users (MUEs) to clusters by max-min criterion, by which each MUE can avoid using the same resource as the nearest femtocell. The third is a novel adaptive power control scheme with femtocells downlink transmit power adjusted adaptively based on the signal to interference plus noise ratio (SINR) level of neighboring users. Simulation results show that the proposed scheme can effectively increase the successful transmission ratio and ergodic capacity of femtocells, while guaranteeing QoS of the macrocell.

Keywords: Femtocell Networks, Interference Mitigation, Clustering, Adaptive Power Control

This work was supported by National Natural Science Foundation of China (No.60972041, 61271234); Ph.D. Program Foundation of Ministry of Education (No.20123223110002); Open Research Foundation of National Mobile Communications Research Laboratory, Southeast University; and the Graduate Innovation Program under Grant CXZZ13_0485.

<http://dx.doi.org/10.3837/tiis.2014.04.015>

1. Introduction

Recently, femtocell technology has drawn considerable attention, which promises to extend cellular coverage and enhance capacity in a cost-effective way [1],[2]. A femtocell is a low-power, low-cost wireless cellular network, deployed by users and connected to the core network by xDSL or optical fiber [3]. It aims at supplying an indoor coverage of small range, such as household and office. Femtocells are expected to benefit both home users and operators. From users' perspective, they can enjoy high-speed and reliable wireless service due to the short distance between the transmitter and receiver, and battery energy can also be conserved. From operators' perspective, because femtocells are purchased and deployed by users, a lot of cost for the operation, management and maintenance is saved. In addition, femtocells can offload the burden from cellular network and subsequently improve network capacity.

However, these benefits are not easy to gain before interference issues are effectively solved [4],[5]. Two main factors lead to serious interference problems: (i) the random and high-density deployment of femtocells. Femtocells are deployed by users in their interests and they are used in a "plug and play" manner. (ii) the cochannel spectrum sharing between femtocells and the macrocell. Due to the scarce availability of spectrum, it is more likely for cellular operators to implement the macrocell and femtocells in a common spectrum [2]. Because of these factors, there are two classes of interference in the system [6]: (i) co-tier interference among femtocells. One femtocell may experience serious interference from others for the dense deployment, although their transmit power is low. (ii) cross-tier interference between femtocells and the macrocell. Due to universal frequency reuse, the transmission of femtocells may cause interference to the macrocell users (MUEs), and vice versa, especially when MUEs are far from the macrocell base station (MBS) and stay in the proximity of femtocells.

Therefore, without effective interference management, both MUEs and femtocell users (FUEs) will experience severe performance deterioration. This paper only considers the downlink scenario and has three objectives: (i) protection of the macrocell's downlink, (ii) protection of femtocells' downlink, (iii) efficient power allocation among femtocells. To achieve these objectives, our paper focuses on successful transmission ratio and capacity analysis of femtocells.

1.1 Related Work

Since the advent of femtocells, the interference problem has been a hot topic in the academic community. There have been many proposals for resolving the interference issues in two-tier femtocell networks, such as by access control [7],[8],[9], spectrum assignment [10],[11],[12], power control [13],[14], coordinated antennas transmission [15], time-slot selection [16], and so on.

Related work also includes [17], which discusses the benefits from dividing the period T into K hopping slots. Each femtocell selects a slot for transmission randomly. It is verified that the interference is "thinned" by the factor K . Our scheme in this paper, in contrast, requires that the distance sum of femtocells using the same slot is maximized by clustering. Though the usage of time slot seems to be with a penalty of reduced capacity, in simulation we find that this structure can improve capacity obviously when the femtocell density is high.

Power control schemes are also used for interference mitigation, which have been

researched in many literatures [18],[19],[20]. In [18], the open-loop and closed-loop power control are used to limit the cross-tier interference to a value less than a threshold. However, co-tier interference is neglected, which is a major factor influencing system performance in high femtocell deployment density. In [19], a distributed interference management architecture---the complementary Tri-control loops---is proposed to determine the femtocells' maximum transmit power based on the feedback of macrocell load margin, and adjust the femtocells' instantaneous transmit power based on their SINRs requirements. However, this scheme is very complex and may not be effective in high femtocell density because it may not be feasible for each femtocell to achieve its required SINR. In [20], it is shown that a feasible power allocation scheme exists for each user to achieve its target SINR if the spectral radius of the normalized channel gain matrix is less than unity. In this scheme, however, channel gains of all links are required for computing the optimal transmit power, which may not be possible in time-varying channel environment and high femtocell density. In our work, in contrast, the power control of a femtocell is based on 1-bit feedback value of its neighboring femtocells and MUEs using the same slot, because the interference in femtocell networks mainly originates from its neighbors. In this way, the femtocell base station (FBS) can adjust its transmit power effectively according to its neighboring users' interference state in a distributed way.

1.2 New Scheme Details

To overcome the limitation of existing proposals, we propose a novel interference mitigation scheme, which includes three steps. Firstly, due to relatively slow variation in the locations and numbers of femtocells after turned on, they are divided into clusters by maximizing the distance sum between femtocells using the same slot. In this way, the interference among femtocells is reduced. Besides, we also prove that an optimal cluster number exists for a certain femtocell deployment density. Secondly, due to fast variation in the locations of MUEs, max-min distance criterion is used to assign MUEs into different femtocell clusters, which ensures that the minimum distance between MUEs and their clusters is maximized in all assignment policies. Each MUE uses the same slot as the cluster that it belongs to. In this way, the worst case that MUEs use the same slot as their nearest femtocells can be avoided. Thirdly, a new distributed power control scheme is proposed to increase the number of femtocells transmitting successfully and make full use of power resource. Every femtocell adjusts transmit power based on its neighbors' responses to its current power. To our best knowledge, the new power control method is firstly developed in femtocell networks. Fig. 1 illustrates more details of the new scheme.

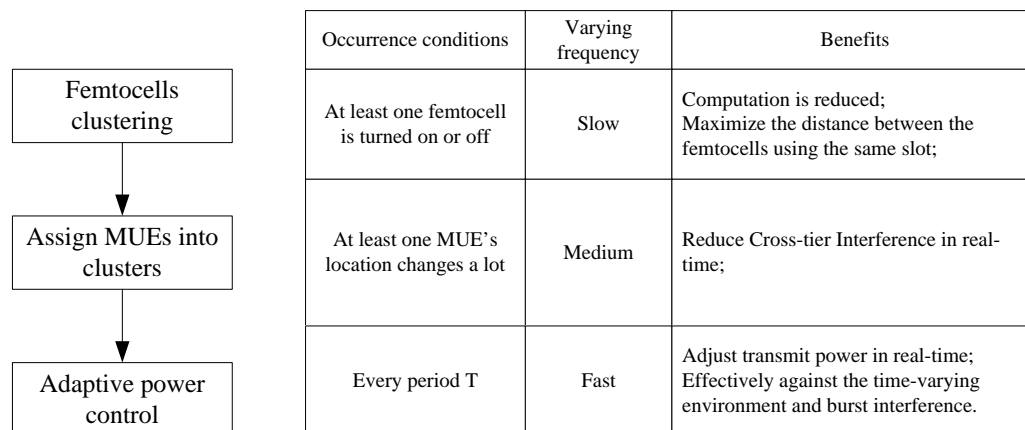


Fig. 1. Overall architecture of the new scheme

The rest of this paper is organized as follows. Section 2 introduces the model of the system. Analysis of clustering of femtocells and MUEs is presented in Section 3. Section 4 describes the adaptive power control algorithm. The simulation results are provided in Section 5. In Section 6, the conclusion is given.

2. System Model and Assumptions

We consider the scenario where a macrocell is underlaid with N cochannel femtocells. The MBS is located at the center, with a cellular coverage radius R , serving M MUEs. FUEs are in the area of their FBS with coverage radius R_f . In this paper, the closed access mode is considered. That is, only authorized subscribers can access the femtocell. For analytical tractability, cochannel interference from neighboring macrocells is ignored.

Assumption 1: The period T is divided into K slots, each duration being T/K . Each MUE and femtocell only choose a slot for transmission, and keep silent in the remaining $K-1$ slots.

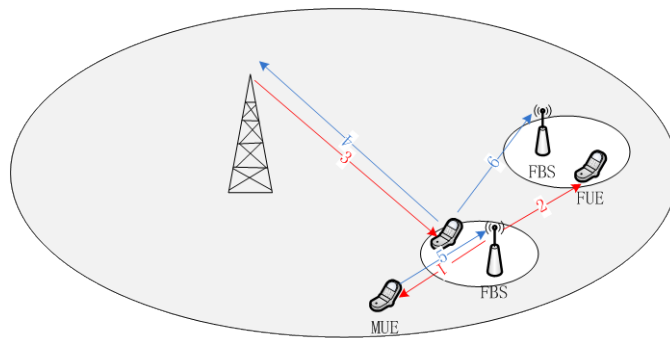
Assumption 2: There is only one scheduled active user per cell (the macrocell and femtocells) per channel during each slot. In this way, intra-cell interference can be avoided.

The channel is represented as a combination of path loss, shadowing effect and wall penetration loss, which is given by

$$h(d) = \begin{cases} K_1 (d_1 / d)^\alpha \Theta_1 & \text{outdoor transmission} \\ K_2 (d_2 / d)^\beta \Theta_2 & \text{indoor transmission} \\ K_1 (d_1 / d)^\alpha \Theta_1 / L_{out} & \text{outdoor to indoor transmission} \\ K_2 (d_2 / d)^\beta \Theta_2 / (2L_m) & \text{indoor to indoor transmission} \end{cases}$$

where $K_i = 20 \log_{10} \lambda / (4\pi d_i)$ is a constant with $d_1=100$ and $d_2=5$, λ is the signal wavelength, α and β are respectively the path loss exponents for outdoor and indoor transmission, Θ_i is the shadowing fading with $10 \log_{10} (\Theta_i) \sim N(0, \sigma_{dB}^2)$ (σ_{dB} is the standard deviation of random lognormal shadowing), L_{out} and L_{in} are respectively outer and interior wall penetration loss, d is the distance between the transmitter and receiver.

We only consider the cochannel interference in this paper. There are six kinds of interference in the system [21], as shown in Fig. 2, and we only focus on the downlink in the two-tier cellular system (the same scheme in Section 3 and 4 may draw different conclusions when applied to uplink).



(a) System model

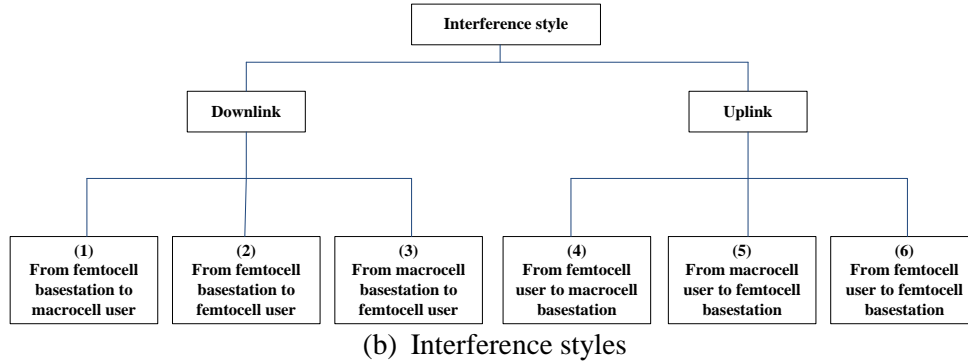


Fig. 2. Cochannel interference in the system

(a) Interference from FBSs to the MUE: Under the expected cochannel femtocell deployment, transmission of femtocells may cause interference to the ongoing transmission of the macrocell using the same slot. What is worse, when the MUE stays far from the MBS and in the proximity of femtocells, the desired signal from the MBS is very weak due to path loss, while the interference from the FBSs is relatively strong due to the short distance between them. Let p_j^f denote the downlink transmit power of FBS j . The channel coefficient between MUE and FBS j is denoted by h_{j0} . And S_m represents the set of femtocells using the same slot with the MUE. Then, interference at the MUE is

$$I_{fm} = \sum_{j \in S_m} p_j^f h_{j0} \quad (1)$$

(b) Interference from FBSs to FUEs: Under high-density deployment of femtocells, the distance between femtocells is short. The FUEs will be subject to interference from other femtocells, especially from neighboring femtocells.

Assumption 3: For small size of femtocells, we assume that the channel coefficient between FBS j and i is approximate to that between FBS j and the active user of FBS i . Due to the existence of wall penetration loss, the assumption is reasonable.

Let h_{ji} denote channel coefficient between FBS j and i . And S_i represents the set of femtocells using the same slot as FBS i . Then, interference at the FUE of femtocell i from other FBSs is

$$I_{ff} = \sum_{j \in S_i, j \neq i} p_j^f h_{ji} \quad (2)$$

(c) Interference from the MBS to FUEs: FUEs will also receive interference from the MBS. In general, this interference is weak, since FBSs are installed in the place where the MBS signal is poor.

Assumption 4: Similar to Assumption 3, because the distance between the MBS and FBS is much larger than that between FBS and users of the FBS, we assume that the channel coefficient between the MBS and an FBS is approximate to that between the MBS and users of the FBS.

Let p_0 denote macrocell downlink transmit power. The channel coefficient between MBS and FBS i is denoted by h_{0i} . Then, interference at the FUE from MBS is

$$I_{mf} = p_0 h_{0i} \quad (3)$$

From the above analysis, signal to interference plus noise ratio (SINR) of the MUE and femtocell i can be expressed as:

$$\gamma_0 = \frac{p_0 h_{00}}{I_{fm} + \sigma^2}, \quad (4)$$

$$\gamma_i = \frac{p_i^f h_{ii}}{I_{mf} + I_{ff} + \sigma^2} \quad (5)$$

respectively, where h_{00} , h_{ii} are the channel coefficients between the MBS and its MUE, and between FBS i and its FUE, respectively, and σ^2 is noise power.

3. Clustering

As we know, interference is caused by the fact that the macrocell and femtocells use the same time-frequency resources. To mitigate interference between them, one effective method is to maximize the distance between users using the same resources. In this section, we cluster femtocells and MUEs respectively based on their movement characteristics. The process is divided into two steps: (i) femtocells clustering, (ii) assigning MUEs into clusters. In the discussion, the frequency band is identical for each user.

3.1 Femtocells Clustering

Once FBSs are turned on, their positions and numbers change relatively slowly. Femtocells are divided into K clusters and all femtocells in the same cluster will transmit in the same slot, and remain silent in the other slots. It must be ensured that the distance between FBSs using the same slot is maximized to minimize interference among them. The clusters will not be reorganized until at least one FBS is turned on or off. The femtocells clustering problem can be described as follows.

$$\begin{aligned} \max \quad & \sum_{l=1}^K \sum_{i,j \in N_l, i \neq j} d_{ij} \\ \text{s.t.} \quad & \bigcup_{l=1}^K N_l = S \\ & N_m \cap N_n = \emptyset; \quad m \neq n, \quad m, n \in [1, K] \\ & N_l \neq \emptyset; \quad l \in [1, K] \\ & \left| |N_m| - |N_n| \right| \leq 1; \quad m \neq n, \quad m, n \in [1, K] \\ & d_{ij} > D \end{aligned} \quad (6)$$

where $d_{ij} = \sqrt{(x_i - x_j)^2 + (y_i - y_j)^2}$ is the distance between FBS i and j which are located at (x_i, y_i) and (x_j, y_j) , N_l and S are the sets of femtocells in cluster l and all femtocells, respectively. The first constraint indicates that all femtocells are assigned into clusters. The second one allows every femtocell to be assigned into only one cluster. The third one represents that every cluster has at least one element, which guarantees that time resource has been fully used. The fourth one shows that the number of femtocells in every cluster is almost identical, where $|N_i|$ denotes the cardinality of set N_i . The last one ensures that the minimum distance between femtocells using the same slot is larger than a certain value, where D is determined by the interference femtocells can bear.

The above analysis is based on $N > K$. When $N \leq K$, the situation is slightly different, where

in order to make full use of time resources, every cluster must contain at least one femtocell, and then one femtocell may be assigned into multiple clusters.

Lemma 1: When the number of clusters $K \geq N$, the co-tier interference is 0. When $K < N$, the interference among femtocells is less than $1/K$ times that without clustering.

The co-tier interference is ‘thinned’ by a factor of K when users choose a slot for transmission randomly [17]. Obviously, the interference will be further reduced by clustering because the distance between femtocells using the same slot is enlarged.

Theorem 1: There exists a value γ^* . If the SINR γ of an FUE is less than γ^* , clustering can increase its average capacity, otherwise the average capacity without clustering is larger.

The proof of Theorem 1 is presented in Appendix I.

Due to the fixed value of the received power in the proof, Theorem 1 can also be expressed as follows.

Theorem 1’: There exists a value I^* . If the interference I to a femtocell is larger than I^* , clustering can increase the average capacity, otherwise the average capacity without clustering is larger.

As we know, the amount of interference is directly proportional to the density of femtocells. The higher is the density of femtocells, the larger is the interference to FUEs. Then, we can get some corollaries.

Corollary 1: In high density of femtocells, the average capacity can be improved by clustering, while in low density of femtocells, the conclusion is opposite.

Because the density of FBSs is inversely proportional to the number of clusters, we can also get corollary 2.

Corollary 2: For a certain number of femtocells, there exists a optimal cluster number K^* ($K^* \geq 1$) with maximum average capacity.

3.2 Assigning MUEs to Clusters

Since MUEs are mobile, their locations may change rapidly. If we cluster MUEs and femtocells simultaneously, the clusters need to be changed quickly, and heavy computation burden will be incurred. Therefore, after femtocells clustering has been completed (the clusters don’t change in a relatively long period of time), we use the max-min criterion to cluster MUEs, so that all MUEs are in a relatively far distance from the FBSs using the same slot. Every MUE uses the same slot as the cluster that it belongs to. In this way, the worst case that the MUE uses the same resource as the nearest femtocell can be avoided.

Definition 1: Let l_{ij} denote the distance between MUE i and cluster j , which is defined as the shortest distance between MUE i and all elements of cluster j , that is, $l_{ij} = \min_{m \in N_j} (d'_{i,m})$, where

$d'_{i,m}$ is the distance between MUE i and the element m of cluster j .

From Assumption 2, we know there are K scheduled MUEs in one channel. Letting A_q denote the assignment policy, the number of all policies is $K!$ ($= K \times (K-1) \times \dots \times 1$). The max-min criterion requires that the minimum distance of all MUEs to their clusters is maximized in all assignment policies. Therefore, MUEs clustering problem can be described as follows.

$$\max_{A_q} \left[\min(l_{ij}) \right] = \max_{A_q} \left[\min(\min_{m \in N_j} (d'_{i,m})) \right] \quad (7)$$

When active MUEs number $M < K$, one MUE may be assigned to multiple clusters in order to make full use of time resource.

4. Adaptive Power Control

After clustering, downlink interference only happens in the same cluster due to using the same time resource. In this section, we only consider one cluster including one MUE and F femtocells.

Due to time-varying environments and bursty interference in two-tier networks [19], we need to control the power of femtocells adaptively in real-time to meet the users' SINR requirements. To research power control of FBSs, three factors need to be considered: (i) as the FBS transmit power is low and wall penetration loss exists, the downlink interference to femtocells and the MUE is mainly from neighboring FBSs using the same slot; (ii) due to the random and high-density deployment of femtocells, distributed power control scheme is preferred; (iii) taking into account the processing capability of the FBSs, the scheme should not involve complex calculations. In this section, a novel power control scheme is proposed based on 1-bit feedback of neighboring users (including the MUE and FUEs). In this new scheme, the MUE and each FBS must obtain their neighboring lists firstly, followed by distributed power control.

4.1 Acquisition of Neighboring Lists

(a) **Obtain neighboring FBSs:** FBS i can send a pilot sequence with a constant power. If the received signal power of the FUE in femtocell j ($j \neq i$) is larger than a certain threshold I_{th} , FBS i will be added to the neighboring list of femtocell j , as shown in Fig. 3(a).

(b) **Obtain the neighboring MUE:** If the MUE receives the femtocell's pilot signal power over a certain threshold, the FBS will be classified as interfering FBS and added to the neighboring list of the MUE. And then, the FBS is reported that the MUE is in the neighboring list of the femtocell by two ways, as shown in Fig. 3(b).

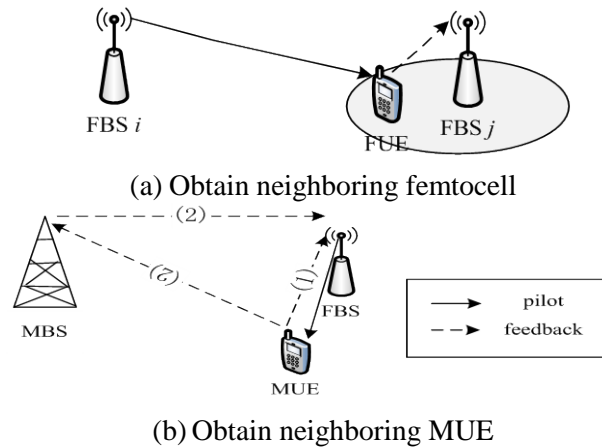


Fig. 3. Acquisition of neighboring list

4.2 Adaptive Power control Scheme

(a) Initialization of FBSs Transmit Power

We assume MBS downlink transmit power is a constant. The goal of this initialization ensures that the SINR of the MUE is larger than a predefined threshold Γ_m , that is,

$$\Gamma_m \leq \frac{P_r}{\sum_{i \in N_m} p_i L_{i0} + N_0} \quad (8)$$

where p_r , p_i , L_{i0} are the received power of the MUE, the transmit power of FBS i in the neighboring list of the MUE and the path loss between the MUE and FBS i , respectively. L_{i0} is the local path loss of MUE and can be estimated by the received power of the constant pilot power of FBS i . For fairness, the initial transmit power of every FBS in one cluster is the same and can be expressed as

$$p_{ini} = \frac{p_r}{\Gamma_m \sum_{i \in N_m} L_{i0}} - \frac{N_0}{\sum_{i \in N_m} L_{i0}} \quad (9)$$

The MUE reports the power level information to all FBSs in the same cluster. Let p_{\max} denote the maximum transmit power of the FBS. The initial transmit power of each FBS should not be in excess of p_{\max} , that is,

$$p_i(1) = \min(p_{\max}, p_{ini}) \quad (10)$$

(b) Three-Level SINR based feedback

Definition 2: The SINR of user i is divided into three zones, as shown in Fig. 4, interference zone $R_1: \gamma_i < \Gamma_i^{(1)}$, acceptable zone $R_2: \Gamma_i^{(1)} \leq \gamma_i < \Gamma_i^{(2)}$ and comfortable zone $R_3: \Gamma_i^{(2)} \leq \gamma_i$.

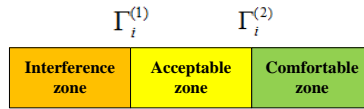


Fig. 4. Interference classification

In our modeling framework, user i ($i > 0$) represents the user of FBS i (for one user/cell/channel/slot according to Assumption 2) and $i=0$ represents the MUE. Accordingly $\Gamma_0^{(1)} = \Gamma_m$, which is used in (8).

User i feeds back a value, which represents the degree of interference according to the received SINR γ_i , to its neighboring femtocells. When $\gamma_i \in R_1$, it informs neighboring femtocells that downlink transmit power needs to be reduced to improve its SINR. When $\gamma_i \in R_3$, it informs neighboring femtocells that downlink transmit power can be increased to make full use of power resource. When $\gamma_i \in R_2$, it reports nothing. Letting $x_i(t)$ denote 1-bit feedback value of user i at time t , then,

$$x_i(t) = \begin{cases} 1; & \gamma_i \in R_3 \\ 0; & \gamma_i \in R_1 \end{cases} \quad (11)$$

Each FBS stops transmission whenever its attained SINR falls below a predefined threshold ($\Gamma_i^{(1)}$) and hasn't increased for a long time. The rationale is that a minimum SINR is required for supporting a minimum data rate and a desired bit error rate. A negligible level of SINR would not help anything at all, but only create unnecessary interference to other users.

So, every FBS has a timer T_i with a initial value 0, which is used to count the times when the SINR of FBS i doesn't increase, keeping below $\Gamma_i^{(1)}$. The timer can be expressed as

$$T_i(t) = \begin{cases} T_i(t-1) + 1; & \gamma_i(t) \leq \gamma_i(t-1) \text{ and } \gamma_i(t) < \Gamma_i^{(1)} \\ 0; & \text{others} \end{cases} \quad (12)$$

When T_i achieves a predefined threshold T_s , the FBS will give up transmission. Therefore, after convergence, an active user i must have $\gamma_i \geq \Gamma_i^{(1)}$.

(c) Calculation Rule of Feedbacks from Neighboring Users

We assume there are n users in the neighboring list of FBS i . It receives $n_i(t)$ feedback values from users in neighboring list at time t , where $n_i(t) \leq n$. That's because users whose SINRs in R_2 feedback nothing. The calculation rule of feedback is as follows.

$$y_i(t) = x_1(t) \otimes x_2(t) \otimes \cdots \otimes x_{n_i(t)}(t) \quad (13)$$

where \otimes is logic AND operation, and the operation rule is as follows: $0 \otimes 0 = 0$, $0 \otimes 1 = 0$, $1 \otimes 0 = 0$, $1 \otimes 1 = 1$.

(d) Iterative Power-Update Rule

The FBS i transmit power is updated using the following iterative rule:

$$p_i(t+1) = \begin{cases} p_i(t) - \Delta p; & y_i(t) = 0 \text{ and } \gamma_i(t) > \frac{p_i(t)}{p_i(t) - \Delta p} \Gamma_i^{(1)} \\ p_i(t) + \Delta p; & y_i(t) = 1 \text{ and } n_i(t) = n \\ p_i(t); & \text{others} \end{cases} \quad (14)$$

where Δp is the granularity of transmit power adjustment.

Since the transmit power of the FBS can't exceed the maximum, the downlink transmit power should be

$$p_i(t+1) = \min(p_i(t+1), p_{\max}) \quad (15)$$

Next, we analyze the iterative power-update rule. To understand the analysis easily, we firstly consider the design of $\Gamma_i^{(2)}$. In the update process, a worst case is that FBS i reduces its transmit power and every FBS in the neighboring list increases their transmit power. To ensure that the SINR of FBS i is above the threshold after this iteration, the following inequality should be true.

$$\frac{p_i(t) - \Delta p}{I_i(t) + \Delta p \sum_{j \in B_i} L_{ji}} > \Gamma_i^{(1)} \quad (16)$$

As the neighboring FBSs increase their transmit power, the SINR of FBS i must be in comfortable zone R_3 . Then, we only need to consider the design of $\Gamma_i^{(2)}$ to ensure that (16) is always true. The analysis of power control process is as follows.

(i) $p_i(t+1) = p_i(t) - \Delta p$. There are two conditions for a FBS to reduce its power. The first is that at least one FBS's SINR in its neighboring list is in R_1 , that is, $y_i(t) = 0$. The second is that its SINR will be above the predefined threshold after the power adjustment. When $\gamma_i(t) \in R_3$, the condition always holds, which has been analyzed above. When $\gamma_i(t) \in R_2$, the following inequality should be true: $\frac{p_i(t) - \Delta p}{I_i(t)} > \Gamma_i^{(1)}$, that is, $\gamma_i(t) > \frac{p_i(t)}{p_i(t) - \Delta p} \Gamma_i^{(1)}$.

(ii) $p_i(t+1) = p_i(t) + \Delta p$. If all FBSs' SINRs in the neighboring list are in comfortable zone (that is, $y_i(t) = 1$ and $n_i(t) = n$), FBS i will increase its transmit power to make full use of power resource.

(iii) $p_i(t+1) = p_i(t)$. If some FBSs' SINRs are in acceptable zone and the others in comfortable zone, FBS i will keep its transmit power unchanged. For detailed working process of the scheme, see [Algorithm 1](#).

Algorithm 1. Adaptive power control of FBS i

Initialization: $p_i(1) = p_{ini}$, $\gamma_i(0) = 0$, $T_i(0) = 0$, $t = 1$.

Repeat

Determine SINR level and its feedback

Measure $\gamma_i(t)$, If $\gamma_i(t) > \Gamma_i^{(2)}$, $x_i(t) = 1$; else if $\gamma_i(t) < \Gamma_i^{(1)}$, $x_i(t) = 0$; end if

If $\gamma_i(t) \leq \gamma_i(t-1)$ and $\gamma_i(t) < \Gamma_i^{(1)}$, $T_i(t) = T_i(t-1) + 1$; else $T_i(t) = 0$; end if

If $T_i(t) = T_s$, $p_i(t) = 0$; break; end if

Receive feedback from neighboring users and calculate them as follows

$$y_i(t) = x_1(t) \otimes x_2(t) \otimes \dots \otimes x_{n_i(t)}(t)$$

Power update process

If $y_i(t) = 0$ and $\gamma_i(t) > \frac{p_i(t)}{p_i(t) - \Delta p} \Gamma_i^{(1)}$, $p_i(t+1) = p_i(t) - \Delta p$;

Else if $y_i(t) = 1$ and $n_i(t) = n$, $p_i(t+1) = p_i(t) + \Delta p$;

Else $p_i(t+1) = p_i(t)$;

End if

Set $t=t+1$, **repeat until** convergence

4.3 Discussion of Convergence

In this subsection, we show the FBS power is convergent in three cases:

Case 1: $p_i(t) = 0$. If the SINR of the user of FBS i can't meet the requirement for a long time, the FBS will stop transmission, which has been analyzed above.

Case 2: $p_i(t) = p_{max}$. If SINRs of all users in FBS i 's neighboring list are always in comfortable zone, the FBS will increase their transmit power continuously. At last, its transmit power will get the maximum value.

Case 3: $p_i(t+1) = p_i(t)$. The above two cases are special cases. In general, the SINRs of some users in FBS i 's neighboring list are in acceptable zone, and others' SINRs are in comfortable zone. The FBS will keep its transmit power unchanged, and then every user achieves a stable SINR.

5. Simulation Results

The testing region is a residential neighborhood of area $100 \times 100 m^2$, the center of which is at a distance of $400m$ to the MBS, as shown in Fig. 5. MUEs are located in this area randomly, with N ($N=10,15,20,25$) cochannel femtocells. FUEs are within the range of $5-10m$ from their FBSs randomly. Other important simulation parameters are shown in Table 1.

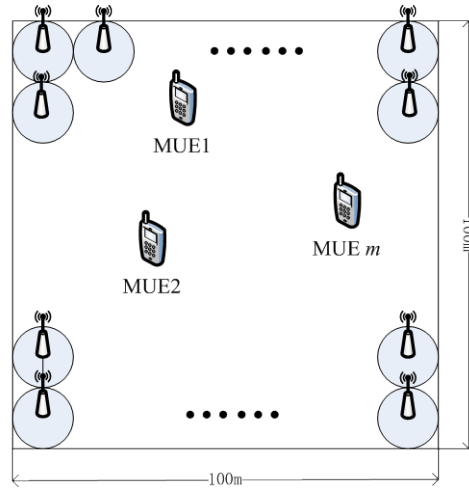


Fig. 5. Testing region

Table 1. Simulation parameters

| Parameter | Value | Parameter | Value |
|--------------------------------------------|-------|-----------------------------------------|--------|
| Macrocell radius R | 500m | Interior wall penetration loss L_{in} | 5dB |
| Femtocell radius R_f | 10m | Antenna pattern | omni |
| Carrier frequency | 2GHz | Noise power [22] | -99dBm |
| Outdoor path loss exponent α | 4 | MBS max transmit power | 43dBm |
| Indoor path loss exponent β | 3 | FBS max transmit power p_{max} | 10dBm |
| shadowing standard deviation σ_{dB} | 4dB | Timer threshold T_s | 5 |
| Outer wall penetration loss L_{out} | 10dB | The granularity Δp | 0.1dBm |
| $\Gamma_i^{(1)}$ | 5dB | $\Gamma_i^{(2)}$ | 8dB |

5.1 The Optimal Clusters Number without Power Control

In this subsection, we only analyze femtocells clustering performance with co-tier interference. We assume all femtocells transmit with the same power. For fair comparison between different clusters numbers, the average capacity is normalized with K , because every femtocell has $1/K$ of time resource to transmit. Hence, the average capacity is expressed as

$$C = \frac{1}{K} \frac{1}{N} \sum_{i=1}^N \log_2(1 + \gamma_i).$$

Fig. 6 shows the average capacity of femtocells with different clusters number K . With the same K , the average capacity decreases as the number of femtocells increases. This is reasonable, as the increase of the number of femtocells results in the increase of aggregated interference to FUEs. Besides, for different femtocell deployment densities, different optimal clusters numbers can be determined in terms of average capacity. In the figure, we can clearly see that the cluster number K with maximum average capacity under femtocell numbers 10, 15, 20, 25 are 3, 3, 4, 5, respectively. The reason is that though clustering reduces the co-tier interference, it also wastes the time resource. That is, when the gain of clustering is less than the loss of time resource, clustering cannot improve the average capacity. So, a tradeoff between them is necessary. The results verify the validity of Theorem 1 and its Corollaries. It is also shown that the superiority of clustering is obvious relative to the scheme without clustering in high femtocells density in terms of average capacity. And the advantage becomes

large as the number of femtocells increases. The reason why the average capacity without clustering is larger than that of $K=3$ and 4 with $N=10$ is that the loss of less transmission time is larger than the gain of less interference brought by clustering as explained above.

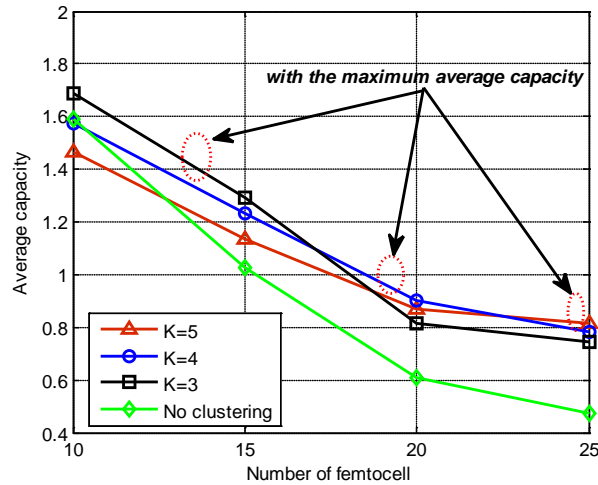


Fig. 6. Average capacity versus femtocell numbers

5.2 Convergence of Power Control Algorithm

The simulation is conducted under the scenario where there are one MUE and five femtocells in one cluster. From Fig. 7, we can see that the MUE’s SINR is always above the predefined threshold (5dB) in the iteration process, because the algorithm is under the condition of ensuring the minimum SINR of the MUE. So, quality of service (QoS) of the MUE can be guaranteed. Besides, we can see that one femtocell’s SINR is below the threshold at the beginning. However, all FUEs’ SINRs are above the predefined threshold (5dB) after convergence, which will increase the number of FUEs with successful transmission. It is also seen that after several iterations the SINRs of FUEs and the MUE achieve stable values in the figure, which shows that FBSs can adapt to the change of environment in real-time.

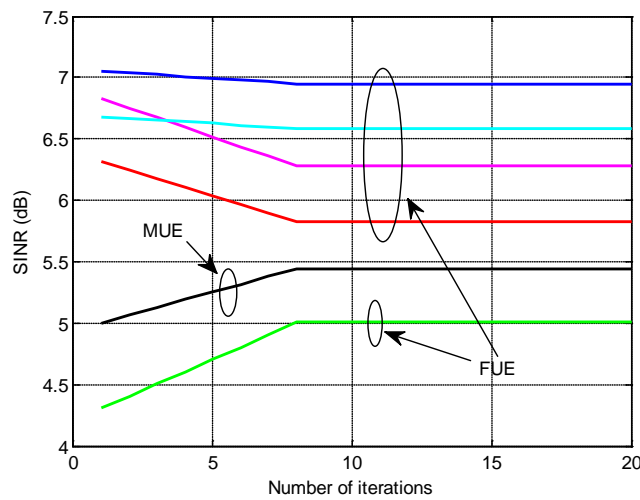


Fig. 7. Convergence of SINR

5.3 System Performance of Femtocells

In this subsection, we analyze the performance of the proposed scheme in terms of successful transmission probability and ergodic capacity. Five algorithms are compared (see [Table 2](#) for details).

Table 2. Five algorithms

| Algorithm | Description |
|------------------------------------------------|---------------------------------------------------------------------------------------------------------------------------------------------------|
| Smart Power Control (SPC) | Every femtocell chooses transmit power based on the received interference, which is proposed by 3GPP [22]. |
| Clustering with Fixed Transmit Power (CFP) | Every femtocell transmits with the fixed power after clustering. |
| Clustering with Power Control (CPC) | Every femtocell adjusts its transmit power adaptively based on feedbacks of its neighboring users. |
| Non-cooperative spectrum solution (Baseline 1) | Each femtocell would plan its subchannels so as to maximize its own capacity without considering others. |
| Cooperative spectrum solution (Baseline 2) | Each FBS gathers information about its neighboring femtocells and performs its subchannels allocation causing less interference to its neighbors. |

Firstly, we define the successful transmission ratio as:

$$\text{successful transmission ratio} = \frac{\text{the number of femtocells whose SINRs are above the predefined threshold } \Gamma_i^{(d)}}{\text{the total number of femtocells } N}$$

[Fig. 8](#) shows the successful transmission ratio of FUEs with different algorithms. The successful transmission ratio of proposed algorithm is obviously better than the others, especially in high femtocell deployment density. We can see when femtocells number $N=25$ and clusters number $K=3$, there is more than 30% improvement in successful transmission ratio of CPC relative to that with SPC or CFP. The reason is that the proposed algorithm can adjust transmit power adaptively based on its neighbors' SINR state in real-time. In addition, the more is the clusters number, the larger is the successful transmission ratio. From the figure, we can see that the successful transmission ratio of $K=5$ is larger than that of $K=3$ and 4, respectively. And all the femtocells can transmit successfully when $K=5$. The reason is obvious. With the increasing of clusters number, the femtocells number in one cluster is reduced and the distance between femtocells in the same cluster is increased. Then, the co-channel interference is reduced considerably. However, this improvement is at the cost of reducing the duration of one transmission slot. Please note that in the schemes of baseline 1 and 2, the spectrum is divided into three subchannels equally. Compared with baseline 1 and 2, clustering can increase the successful transmission ratio of femtocell users when the number of clusters equals that of subchannels. That's because the clustering maximizes the distance between femtocells using the same resources, while baseline 1 selects subchannels selfishly without considering interference to other femtocells and baseline 2 can't guarantee the distance between femtocells using the same resource to be maximized because of taking into account its neighbors spectrum allocation only.

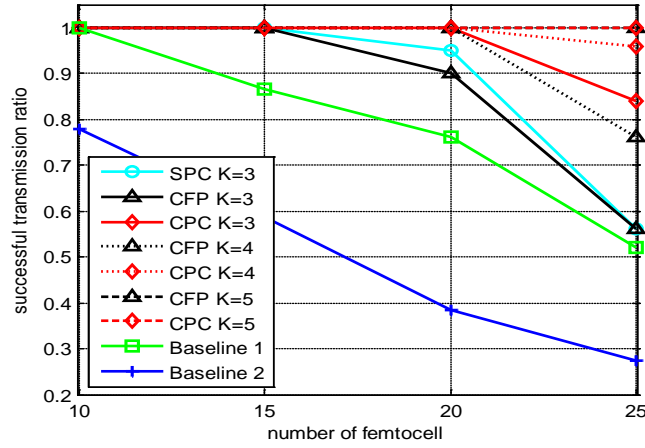


Fig. 8. Successful transmission ratio versus femtocell numbers

Secondly, ergodic capacity is investigated in this part. Similarly, the capacity is normalized by K for fairness among different clusters numbers. The ergodic capacity is defined as $C_i = \frac{1}{K} \frac{1}{N} \sum_{i=1}^N \int_{\Gamma_i^{(1)}}^{+\infty} \log_2(1 + \gamma_i) p(\gamma_i) d\gamma_i$.

Ergodic capacity curves for different algorithms are plotted in Fig. 9. Ergodic capacity decreases with femtocell number increasing, as the co-tier interference increases. The proposed CPC scheme has superiority to the others, especially in high femtocell density. As we can see, when femtocell numbers $N \leq 20$, the performance of CPC is better than SPC slightly. However, the improvement is up to 0.2 bit/s/Hz when $N=25$, which shows the advantage of the proposed scheme is obvious in high femtocell deployment density. Besides, there is also an optimal cluster number for a specific femtocell number in terms of ergodic capacity, which is similar to the explanation of Section 5.1. In addition, the ergodic capacity with clustering is larger than that of baseline 1 and 2. That's because by clustering the interference is reduced more and the number of femtocells with effective transmission ($\text{SINR} \geq \Gamma_i^{(1)}$) is larger. Therefore, the effective quantity contributing to ergodic capacity is larger according to its definition above. Combining Fig.8 and Fig. 9, we get that the proposed CPC scheme can improve the system performance in terms of ergodic capacity and successful transmission ratio, especially when the femtocell density is large.

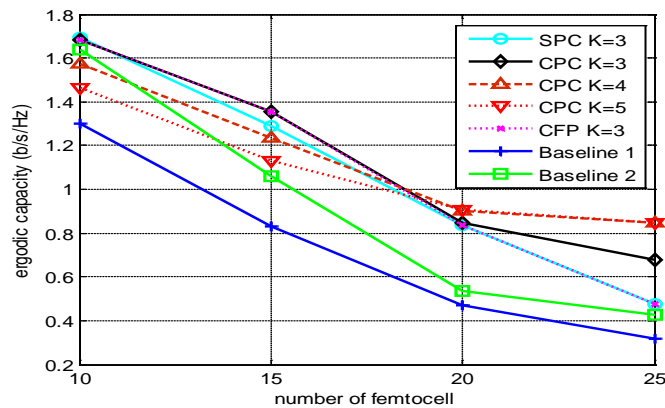


Fig. 9. Ergodic capacity versus femtocell numbers

6. Conclusion

This paper has presented a novel interference mitigation scheme for cochannel two-tier networks. Firstly, based on movement characteristics, we cluster femtocells and MUEs respectively. Simulation results show that clustering can significantly reduce the co-tier interference. Besides, to further improve system performance, we also propose a distributed power control strategy based on the fact that main interference originates from neighbors. At last, we analyze the system downlink performance in terms of successful transmission ratio and ergodic capacity. Extensive simulation results demonstrate that without degrading QoS of the macrocell the proposed scheme can not only increase the successful transmission ratio greatly, but also improve the ergodic capacity of femtocells, especially in high femtocell deployment density.

Appendix I (Proof of Theorem 1)

We assume that the received power of the FUE is p and interference is I . The noise power is ignored in this discussion since it is much less than the interference. Then, the capacity without clustering is $C = \log_2(1 + p/I)$. Assuming that femtocells are divided into K clusters, the average capacity is $C' = (1/K) \log_2(1 + f(K) \cdot p/I)$ because each user has only one slot to transmit after clustering.

Because the interference power of clustering is less than $1/K$ times that without clustering by Lemma 1, then we have

$$f(K) > K \tag{I.1}$$

Let $\gamma = p/I$, then we can get

$$C' - C = \frac{\log_2(1 + f(K) \cdot \gamma) - K \cdot \log_2(1 + \gamma)}{K} = \frac{\log_2(1 + f(K)\gamma) - \log_2(1 + \gamma)^K}{K} \tag{I.2}$$

Let $\varphi(\gamma) = (1 + f(K)\gamma) - (1 + \gamma)^K$, then it can be expressed as follows.

$$\varphi(\gamma) = 1 + f(K)\gamma - (1 + C_K^1\gamma + C_K^2\gamma^2 + \dots + C_K^K\gamma^K) = [f(K) - K]\gamma - C_K^2\gamma^2 - \dots - C_K^K\gamma^K \tag{I.3}$$

where $C_K^i = \binom{K}{i} = \frac{K!}{i!(K-i)!}$.

Let $\phi(\gamma)$ be first order derivative of $\varphi(\gamma)$, then we have

$$\phi(\gamma) = \varphi'(\gamma) = [f(K) - K] - \sum_{i=2}^K i \cdot C_K^i \cdot \gamma^{i-1} \tag{I.4}$$

From (I.1) and (I.4), we can get $\phi(0) = f(K) - K > 0$ and $\phi(+\infty) = -\infty < 0$. Because $\phi(\gamma)$ decreases monotonically, there exists and only exists a value $\gamma_0 (\gamma_0 > 0)$ with $\phi(\gamma_0) = 0$. Then we can get

$$\begin{cases} \phi(\gamma) > 0; & \gamma < \gamma_0 \\ \phi(\gamma) < 0; & \gamma > \gamma_0 \end{cases} \tag{I.5}$$

Based on (I.5), we know that

$$\begin{cases} \varphi(\gamma) \text{ increases monotonically, } & \gamma < \gamma_0 \\ \varphi(\gamma) \text{ decreases monotonically, } & \gamma > \gamma_0 \end{cases} \tag{I.6}$$

For $\varphi(0) = 0$, the value of function $\varphi(\gamma)$ is shown in **Fig. 10**, where $\varphi(\gamma^*) = 0$.

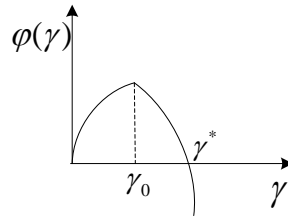


Fig. 10. The value of $\varphi(\gamma)$ relative to γ

Then, we have

$$\begin{cases} \varphi(\gamma) > 0; & \gamma < \gamma^* \\ \varphi(\gamma) < 0; & \gamma > \gamma^* \end{cases} \Rightarrow \begin{cases} \log_2(1 + f(K)\gamma) > \log_2(1 + \gamma)^K; & \gamma < \gamma^* \\ \log_2(1 + f(K)\gamma) < \log_2(1 + \gamma)^K; & \gamma > \gamma^* \end{cases} \Rightarrow \begin{cases} C' > C; & \gamma < \gamma^* \\ C' < C; & \gamma > \gamma^* \end{cases}. \quad (I.7)$$

Reference

- [1] D. Knisely, T. Yoshizawa, & F. Favichia, "Standardization of Femtocells in 3GPP," *IEEE Communications Magazine*, 47, pp. 68-75, 2009. [Article \(CrossRef Link\)](#)
- [2] V. Chandrasekhar, J. Andrews, & A. Gatherer, "Femtocell Networks: A Survey," *IEEE Communications Magazine*, 46, pp. 59-67, 2008. [Article \(CrossRef Link\)](#)
- [3] H. Claussen, L. Ho, & L. Samuel, "An Overview of the Femtocell Concept," *Bell Labs Technical J.*, 13, pp. 221-245, 2008. [Article \(CrossRef Link\)](#)
- [4] T. Zahir, K. Arshad, A. Nakata, K. Moessner, "Interference Management in Femtocells," *IEEE Communications Surveys & Tutorials*, 15, pp. 293-311, 2013. [Article \(CrossRef Link\)](#)
- [5] J. Andrews, H. Claussen, M. Dohler, S. Rangan, & M. Reed, "Femtocells: Past, Present, and Future," *IEEE Journal on Selected Areas in Communications*, 30, pp. 497-508, 2012. [Article \(CrossRef Link\)](#)
- [6] H. Claussen, "Performance of macro- and co-channel femtocells in a hierarchical cell structure," in *Proc. of IEEE 18th International Symposium on Personal, Indoor and Mobile Radio Communications*, 2007. [Article \(CrossRef Link\)](#)
- [7] G. de la Roche, A. Valcarce, D. Lopez-Perez & J. Zhang, "Access Control Mechanisms for Femtocells," *IEEE Communications Magazine*, 48, pp. 33-39, 2010. [Article \(CrossRef Link\)](#)
- [8] P. Xia, V. Chandrasekhar & J. Andrews, "Open vs. Closed Access Femtocells in the Uplink," *IEEE Transactions on Wireless Communications*, 9, pp. 3798-3809, 2010. [Article \(CrossRef Link\)](#)
- [9] H. Jo, P. Xia & J. Andrews, "Downlink Femtocell Networks: Open or Closed?," in *Proc. of IEEE International Conference on Communications (ICC)*, 2011. [Article \(CrossRef Link\)](#)
- [10] D. Lopez-Perez, A. Valcarce, G. de la Roche & J. Zhang, "OFDMA Femtocells: A Roadmap on Interference Avoidance," *IEEE Communications Magazine*, 47, pp. 41-48, 2009. [Article \(CrossRef Link\)](#)
- [11] V. Chandrasekhar & J. Andrews, "Spectrum Allocation in Tiered Cellular Networks," *IEEE Transactions on Communications*, 57, pp. 3059-3068, 2009. [Article \(CrossRef Link\)](#)
- [12] C. Oh, M. Chung, H. Choo, T. Lee, "Resource Allocation with Partitioning Criterion for Macro-Femto Overlay Cellular Networks with Fractional Frequency Reuse," *Wireless Pers Commun*, 68, pp. 417-432, 2013. [Article \(CrossRef Link\)](#)
- [13] X. Li, L. Qian & D. Kataria, "Downlink Power Control in Co-Channel Macrocell Femtocell Overlay," in *Proc. of 43rd Annual Conference on Information Sciences and Systems*, 2009. [Article \(CrossRef Link\)](#)
- [14] H. Wang, R. Song, "Distributed Q-Learning for Interference Mitigation in Self-Organised Femtocell Networks: Synchronous or Asynchronous?," *Wireless Personal Communications*, 71, pp. 2491-2506, 2013. [Article \(CrossRef Link\)](#)
- [15] Y. Li, Z. Feng, D. Xu, Q. Zhang, & H. Tian, "Optimisation approach for femtocell networks using coordinated multipoint transmission technique," *Electronics Letters*, 47, pp. 1348-1349, 2011.

- [Article \(CrossRef Link\)](#)
- [16] K. Meerja, P. Ho & B. Wu, "A Novel Approach for Co-Channel Interference Mitigation in Femtocell Networks," in *Proc. of IEEE Global Telecommunications Conference (Globecom 2011)*, 2011. [Article \(CrossRef Link\)](#)
- [17] V. Chandrasekhar & J. Andrews, "Uplink Capacity and Interference Avoidance for Two-Tier Femtocell Networks," *IEEE Transactions on Wireless Communications*, 8, pp. 3498-3509, 2009. [Article \(CrossRef Link\)](#)
- [18] H. Jo, C. Mun, J. Moon & J. Yook, "Interference Mitigation Using Uplink Power Control for Two-Tier Femtocell Networks," *IEEE Transactions on Wireless Communications*, 8, pp. 4906-4910, 2009. [Article \(CrossRef Link\)](#)
- [19] J. Yun & K. Shin, "Adaptive Interference Management of OFDMA Femtocells for Co-Channel Deployment," *IEEE Journal on Selected Areas in Communications*, 29, pp. 1225-1241, 2011. [Article \(CrossRef Link\)](#)
- [20] V. Chandrasekhar, J. Andrews, T. Muharemovic, Z. Shen & A. Gatherer, "Power Control in Two-Tier Femtocell Networks," *IEEE Transactions on Wireless Communications*, 8, pp. 4316-4328, 2009. [Article \(CrossRef Link\)](#)
- [21] K. Zheng, Y. Wang, W. Wang, M. Dohler & J. Wang, "Energy-Efficient Wireless in-Home: The Need for Interference-Controlled Femtocells," *IEEE Wireless Communications*, 18, pp. 36-44, 2011. [Article \(CrossRef Link\)](#)
- [22] 3GPP. 3GPP TR 36.921 evolved universal terrestrial radio access (EUTRA); FDD home eNode B (HeNB) radio frequency (RF) requirements analysis. 3GPP. Tech. Rep. 2010. [Article \(CrossRef Link\)](#)



Hong Wang received the B.S. degree from Jiangsu University in 2011 and now he is pursuing his study for Ph.D. degree at Nanjing University of Posts and Telecommunications (NUPT). His research interests are in the area of broadband wireless communications.



Rongfang Song received the B.S. and M.S. degree from Nanjing University of Posts and Telecommunications (NUPT) in 1984 and 1989, respectively, and the Ph.D. degree from Southeast University (SEU) in 2001, all in Telecommunications Engineering. From 2002–2003, he was a Research Associate at the Department of Electronic Engineering, City University of Hong Kong. Since 2002, he has been a Professor in the Department of Telecommunications Engineering at NUPT. His research interests include broadband wireless communications, spread-spectrum digital communications, and space-time signal processing.